



**HAL**  
open science

## Engineered covalent leucotoxin heterodimers form functional pores: insights into S–F interactions

Olivier R. Joubert, Gabriella Viero, Daniel Keller, Eric Martinez, Didier A Colin, Henri Monteil, Lionel Mourey, Mauro Dalla serra, Gilles Prévost

### ► To cite this version:

Olivier R. Joubert, Gabriella Viero, Daniel Keller, Eric Martinez, Didier A Colin, et al.. Engineered covalent leucotoxin heterodimers form functional pores: insights into S–F interactions. *Biochemical Journal*, 2006, 396 (2), pp.381 - 389. 10.1042/bj20051878 . hal-03003436

**HAL Id: hal-03003436**

**<https://hal.science/hal-03003436>**

Submitted on 20 Nov 2020

**HAL** is a multi-disciplinary open access archive for the deposit and dissemination of scientific research documents, whether they are published or not. The documents may come from teaching and research institutions in France or abroad, or from public or private research centers.

L'archive ouverte pluridisciplinaire **HAL**, est destinée au dépôt et à la diffusion de documents scientifiques de niveau recherche, publiés ou non, émanant des établissements d'enseignement et de recherche français ou étrangers, des laboratoires publics ou privés.

# Engineered covalent leucotoxin heterodimers form functional pores: insights into S–F interactions

Olivier JOUBERT\*, Gabriella VIERO†, Daniel KELLER\*, Eric MARTINEZ\*, Didier A. COLIN\*, Henri MONTEIL\*, Lionel MOUREY‡, Mauro DALLA SERRA† and Gilles PRÉVOST\*<sup>1</sup>

\*Laboratoire de Physiopathologie et d'Antibiologie Microbiennes, EA 3432, Institut de Bactériologie de la Faculté de Médecine (Université Louis Pasteur), Hôpitaux Universitaires de Strasbourg, 3 rue Koeberlé, F-67000 Strasbourg, France, †ITC and CNR-IBF Unit at Trento, 18 Via Sommarive, I-38050 Povo (Trento), Italy, and ‡Groupe de Biophysique Structurale, Département Mécanismes Moléculaires des Infections Mycobactériennes, CNRS-IPBS UMR 5089, 205 route de Narbonne, F-31077 Toulouse Cedex, France

The staphylococcal  $\alpha$ -toxin and bipartite leucotoxins belong to a single family of pore-forming toxins that are rich in  $\beta$ -strands, although the stoichiometry and electrophysiological characteristics of their pores are different. The different known structures show a common  $\beta$ -sandwich domain that plays a key role in subunit–subunit interactions, which could be targeted to inhibit oligomerization of these toxins. We used several cysteine mutants of both HlgA ( $\gamma$ -haemolysin A) and HlgB ( $\gamma$ -haemolysin B) to challenge 20 heterodimers linked by disulphide bridges. A new strategy was developed in order to obtain a good yield for S–S bond formation and dimer stabilization. Functions of the pores formed by 14 purified dimers were investigated on model membranes, i.e. planar lipid bilayers and large unilamellar vesicles, and on target cells, i.e. rabbit and human red blood cells and polymorpho-

nuclear neutrophils. We observed that dimers HlgA T28C–HlgB N156C and HlgA T21C–HlgB T157C form pores with similar characteristics as the wild-type toxin, thus suggesting that the mutated residues are facing one another, allowing pore formation. Our results also confirm the octameric stoichiometry of the leucotoxin pores, as well as the parity of the two monomers in the pore. Correctly assembled heterodimers thus constitute the minimal functional unit of leucotoxins. We propose amino acids involved in interactions at one of the two interfaces for an assembled leucotoxin.

**Key words:** assembly intermediate,  $\beta$ -barrel, intermolecular disulphide bond, pore-forming toxin, protein–protein interaction, *Staphylococcus aureus*.

## INTRODUCTION

PVL (Panton–Valentine leucocidin) and Hlg ( $\gamma$ -haemolysin) are bicomponent leucotoxins of *Staphylococcus aureus* which form pores in blood cell and purely lipid membranes. Components of a leucotoxin sequentially bind to target cells: a class S protein (LukS-PV or HlgA, 32 kDa) first binds the surface of leucocytes and then, a class F protein (LukF-PV or HlgB, 34 kDa) interacts to develop a bipartite oligomeric and cytolytic pore [1]. *S. aureus*  $\alpha$ -toxin and leucotoxins belong to the family of the  $\beta$ -barrel pore-forming toxins. This family includes other members, such as the aerolysin from *Aeromonas hydrophila*, the *Vibrio cholerae* cytotoxin, leucotoxins from *Clostridium septicum* and cholesterol-dependent cytotoxins, such as PFO (perfringolysin O) from *Clostridium perfringens* [2]. This family also includes compounds that have a role as translocation subunits, such as the anthrax protective antigen from *Bacillus anthracis* [3], and the iota-toxin from *Clostridium perfringens* [4]. All of these toxins have three common features. They are rich in  $\beta$ -strands, they have no hydrophobic stretch and full oligomerization is a prerequisite. *S. aureus*  $\alpha$ -toxin forms non-lytic prepores before undergoing conformational changes leading to pore formation [5–8], as do several related toxins [9–14]. Oligomerization occurs near to or on the membrane surface before insertion, rather than by lateral addition of monomers already inserted [15].

As they often are associated with pathologies [1], the characterization of protein–protein interactions mainly constitutes an important step towards the inhibition of oligomerization of pore-forming toxins and the understanding of the molecular dynamics

leading to pore formation. In the case of PFO, the monomer binding to cholesterol-containing membranes, it induces some allosteric modifications occurring at a structural element (strand  $\beta 5$ ) to move and to expose the edge of a previously hidden  $\beta$ -strand ( $\beta 4$ ) that participates in the protomer–protomer interaction via hydrogen bonding of strand  $\beta 1$  of a given monomer to the now-exposed strand  $\beta 4$  in the original PFO dimer [16]. The oligomer assembly is obtained through productive collisions of the previously inserted monomers. Up to 50 PFO molecules assemble in a circular prepore complex [12]. Finally, there is a co-operative insertion of the transmembrane  $\beta$ -hairpins into the membrane to form a large pore [17]. HlgA and HlgB bind to membranes as monomers [18]. Until now, the stoichiometry of the leucotoxin pore has been controversial, with heptamers suggested by electron microscopy [19], or octamers identified by the analysis of labelled or covalently linked proteins [20,21], but hexamers were also proposed [22]. An HlgA–HlgB dimer contains an equimolar ratio of the two proteins [22], and FRET (fluorescence resonance energy transfer) experiments have demonstrated the alternative location of the two proteins in the pore [23]. Furthermore, slight modifications occur in the secondary structure during the prepore formation [22] that may favour protein–protein interactions [24]. Valeva et al. [25] demonstrated that a co-operative assembly between  $\alpha$ -toxin protomers occurs during prepore formation. In the present study, several purified heterodimers of HlgA–HlgB were obtained by disulphide bonding via mutagenesis. Biological activities and characteristics of the pores for dimers and WT (wild-type) toxin were compared using different membrane systems to gain insights into monomer S–monomer F interactions.

Abbreviations used: DTDP, 2,2'-dithiodipyridine; DTT, dithiothreitol; GST, glutathione S-transferase; Hlg,  $\gamma$ -haemolysin; HRBC, human red blood cell; LUV, large unilamellar vesicle; PEG, poly(ethylene glycol); PFO, perfringolysin O; PMN, polymorphonuclear neutrophil; PVL, Panton–Valentine leucocidin; RRBC, rabbit red blood cell; WT, wild-type.

<sup>1</sup> To whom correspondence should be addressed (email gilles.prevast@medecine.u-strasbg.fr).

## MATERIALS AND METHODS

### Bacterial strains, vector and site-directed mutagenesis

*Escherichia coli* XL1 Blue cells {*recA1 endA1 gyrA96 thi1 hsdR17 supE44 relA1 lac* [F' *proAB lacI<sup>q</sup>ΔM15 Tn10 (tet<sup>r</sup>)*]} (Stratagene) were used as recipient cells for transformation with recombinant pGEX-6P-1<sup>®</sup> control plasmids or following site-directed mutagenesis. *E. coli* BL21 [F<sup>-</sup>, *ompT*, *hsdS* (*rB<sup>-</sup>*, *mB<sup>-</sup>*), *gal*] was used for overexpression of the GST (glutathione S-transferase)–leucotoxin fusion *HlgA* and *HlgB* genes (GenBank<sup>®</sup> accession numbers L01055 and X81586), according to the manufacturer's instructions (Amersham Biosciences) [26,27]. The different mutants were obtained by using dedicated oligonucleotides in a two-step mutagenesis procedure similar to QuikChange<sup>®</sup> mutagenesis (Stratagene), except that Tfu DNA polymerase<sup>®</sup> (Finnzymes) and T4 GP32 protein<sup>®</sup> (Qbiogene) were used instead of Pfu Turbo<sup>®</sup> DNA polymerase.

### Protein purification

Recombinant HlgA was affinity-purified by glutathione–Sephacrose 4B chromatography, followed, after cleaving the GST tag with PreScission<sup>®</sup> protease (Amersham Biosciences), by cation-exchange MonoS<sup>®</sup> FPLC chromatography (Amersham Biosciences) using a NaCl gradient from 0.36 to 0.6 M [26]. It was eluted at approx. 0.51 M NaCl. Recombinant HlgB was purified by hydrophobic interaction chromatography (Resource ISO<sup>®</sup>; Amersham Biosciences) using a (NH<sub>4</sub>)<sub>2</sub>SO<sub>4</sub> gradient ranging from 0.96 to 0.36 M [27], and it was eluted at 0.6 M (NH<sub>4</sub>)<sub>2</sub>SO<sub>4</sub>. All dimer preparations were first adjusted to 1.2 M (NH<sub>4</sub>)<sub>2</sub>SO<sub>4</sub>, before being applied to a hydrophobic interaction chromatography column using the (NH<sub>4</sub>)<sub>2</sub>SO<sub>4</sub> gradient as above. Materials that were eluted at 0.6 M were diluted 1:6 in 0.05 M Na<sub>2</sub>HPO<sub>4</sub>, pH 7.0, to decrease the (NH<sub>4</sub>)<sub>2</sub>SO<sub>4</sub> concentration and were purified further using cation-exchange chromatography as described above. Proteins were then dialysed at 4 °C overnight against 0.02 M Hepes and 0.5 M NaCl, pH 7.5. Controls for homogeneity were performed using SDS/10–15% PAGE, and the proteins were then stored in the presence of 1 mM DTT (dithiothreitol) at –80 °C.

### Dimer synthesis and purification

In order to limit any oxidation of the thiol groups of the cysteine mutants, all buffers were flushed with nitrogen for 30 min. Cysteine mutants of HlgB were first reduced in the presence of 20 mM DTT, desalted by gel filtration on PD10<sup>®</sup> columns (Amersham Biosciences) against 0.05 M Hepes, 0.5 M NaCl, 1 mM sodium EDTA and 0.25 mM DTT, pH 7.5, before being activated with 2.5 mM DTDP (2,2'-dithiodipyridine) for 10 min at room temperature (25 °C). To remove excess DTDP, the activated toxins were desalted for a second time under the same conditions as above. Concurrently, cysteine mutants of HlgA were first desalted by gel filtration on PD10<sup>®</sup> columns against 0.02 M sodium acetate, 0.5 M NaCl and 1 mM sodium EDTA, pH 5.0. The two partners were then mixed for 3 h at 23 °C at a ratio of HlgB Cys–TP/HlgA Cys of 1.5, after the pH was adjusted to 7.5 using 0.5 M Bicine, pH 9.0 (15 mM final concentration). Finally, mixtures were adjusted to 0.5 mM DTDP to block the residual free thiol groups, and before further purification of heterodimers as indicated above. For testing the residual accessibility of free thiols, approx. 30 nmol of proteins in 0.5 ml were pelleted by centrifugation at 5000 g for 10 min in 5% (w/v) trichloroacetic acid and left for 5 min at 0 °C, before being washed three times with the same solution. The precipitate was dissolved in 400 μl of N<sub>2</sub>-saturated 0.2 M Hepes,

0.2 M NaCl and 1 mM sodium EDTA, pH 8.0, and was used for a direct Ellman's titration [28].

### Planar lipid bilayer experiments

Planar lipid bilayers were prepared by the application on both sides of a 0.1 mm hole in a 12 μm Teflon foil (pre-treated with n-hexadecane) of two monolayers of 99% pure diphytanoyl phosphatidylcholine (Avanti Polar Lipids) spread from a 5 mg · ml<sup>-1</sup> solution in pentane. Toxins were added on one side (*cis*) to stable pre-formed bilayer. All experiments were started in symmetrical solutions (10 mM Hepes, 100 mM KCl, and 0.1 mM sodium EDTA, pH 7.0). Macroscopic currents were recorded on a patch clamp amplifier (Axopatch 200<sup>®</sup>; Axon Instruments). A computer equipped with a DigiData 1200 A/D converter (Axon Instruments) was used for data acquisition. The current traces were filtered at 0.1 kHz and acquired by computer assistance using Axoscope 8 software (Axon Instruments). Measurements were performed at room temperature as described previously [29].

### Permeabilization of lipid vesicles by leucotoxins

For calcein (Sigma) release experiments, LUVs (large unilamellar vesicles) were prepared by extrusion of 3 mg/ml phosphatidylcholine/choline at a 1:1 molar ratio, as described previously [30]. LUVs were washed on Sephadex G-50 medium pre-equilibrated with 20 mM Tris/HCl, 20 mM NaCl and 0.1 mM EDTA, pH 7.0. Permeabilization was assayed using a fluorescence microplate reader. Each well contained LUVs (7 μm lipid) and various leucotoxin dilutions. The two components were applied at equimolar concentration in 200 μl of 20 mM Tris/HCl, 20 mM NaCl and 0.1 mM EDTA, pH 7.0. Maximal protein concentration was 5 nM with HlgB plus HlgA, 50 nM with heterodimers.

### Human PMNs (polymorphonuclear neutrophils) and flow cytometry measurements

Human PMNs from healthy and anonymous donors were purified from buffy coats obtained from a blood bank [EFS (Etablissement Français du Sang), Strasbourg, France] as reported previously [31] and were resuspended in 10 mM Hepes, 140 mM NaCl, 5 mM KCl, 10 mM glucose and 0.1 mM EGTA, pH 7.3, at 5 × 10<sup>5</sup> cells/ml. Flow cytometry was carried out using a FacSort<sup>®</sup> flow cytometer (Becton-Dickinson) equipped with an argon laser tuned to 488 nm [27]. Intracellular calcium was evaluated using flow cytometry of cells loaded previously with 5 μM Fluo-3 (Molecular Probes) in the presence of 1.1 mM extracellular Ca<sup>2+</sup>. Pore formation and univalent cation influx were revealed by the penetration of ethidium bromide into the pores; cells were incubated for 30 min with 4 μM ethidium bromide before toxin addition in the absence of extracellular Ca<sup>2+</sup>. Fluo-3 and ethidium bromide fluorescence was measured using Cell Quest Pro<sup>™</sup> software (Becton-Dickinson) [27,31]. Results from at least four different donors were averaged and expressed as percentages of control of human PMNs treated with HlgA–HlgB. Base level values were obtained for each series of data from a control without addition of toxin. These were systematically subtracted from the other assays. S.D. values never exceeded 10% of the obtained values and were removed from the Figures for clarity.

The dissociation constant ( $k_{d[*S*]}$ ) of HlgA for the PMN membrane and that of HlgB for the PMN membrane-bound HlgB ( $k_{d[*F*]}$ ) were reported previously to be 2 nM and 0.04 nM respectively [32]. WT and mutants of HlgA were applied at 20 nM, whereas WT and mutants of HlgB were applied at 0.4 nM. The heterodimers were applied at 20 nM.

### Determination of pore radii

The radii of pores formed by native and modified leucotoxins were assessed using flow cytometry by determining the relative ability of PEG [poly(ethylene glycol)] molecules of various sizes to protect cells from osmotic leakage as described previously [33]. HlgA and HlgB (each at 20 nM), or 20 nM of heterodimers were mixed with 30 mM PEG polymers of different aqueous pore radii (0.94, 1.12, 1.22 and 1.44 nm), incubated for 40 min, before forward side scatter values were collected at 0, 10, 20 and 30 min after toxin application [26].

### Haemolysis assays

HRBCs (human red blood cells) were retrieved from buffy coats used for PMN preparations (see above). They were first pelleted by centrifugation at 1000 *g* for 5 min, then washed three times in PBS (10 mM NaH<sub>2</sub>PO<sub>4</sub>, 1.5 mM Na<sub>2</sub>HPO<sub>4</sub> and 0.15 M NaCl, pH 7.0), and finally resuspended in this buffer at 1% (v/v) concentration. Kinetics of haemolysis were carried out at room temperature in a 0.1% (v/v) suspension of HRBCs, which corresponds to an *A*<sub>650</sub> of 1. We measured the decay of *A*<sub>650</sub> every 30 s over 12 min. Complete haemolysis was obtained after 10 min of incubation of 20 nM HlgA and 20 nM HlgB. Measurements were carried out using a Camspec M330 spectrophotometer. The activities of the heterodimers were tested also on RRBCs (rabbit red blood cells) obtained from fresh rabbit blood. Haemolytic activity was determined following the turbidity at 650 nm in a 96-well microplate reader (UVmax; Molecular Devices) for 45 min as described previously [22].

### Identification of oligomers

Oligomers formed in solution or on to human PMN membranes by WT HlgA and HlgB and heterodimers were examined using SDS/3–8% PAGE and immunoblotting. For investigations of oligomers in solution, 4 ng of each toxin component was incubated with 0.3 or 3 mM glutaraldehyde as described below. Preparations of 5 × 10<sup>7</sup> cells/ml in 10 mM Hepes, 140 mM NaCl, 5 mM KCl, 10 mM glucose and 0.1 mM EGTA, pH 7.3, were incubated with 100 nM of LukS-PV, LukF-PV or derivatives in the presence of 10 μl/ml mammalian cell-tissue antiprotease cocktail (Sigma). After a 45 min incubation at 22 °C, biological activity was evaluated by optical microscopy as swelling of the cells and rounding of the nuclei. The cells were washed twice and then resuspended in 1 ml of the same buffer and 1 μl/ml antiprotease cocktail as above. The cells were ground using a FastPrep<sup>®</sup> apparatus (Qbiogene) in FastPrep Blue<sup>®</sup> tubes with orbital centrifugation at 3500 *g* for 10 s at room temperature. The membranes were harvested by ultracentrifugation at 22000 rev./min for 20 min at 4 °C in a TLA rotor. Membrane pellets were resuspended in 100 μl of the same buffer containing 1% (w/v) saponin (Sigma) and 2 μl of antiprotease, incubated for 30 min at room temperature and then centrifuged at 25000 rev./min for 30 min in a TLA rotor. The supernatants were adjusted to 1 mM glutaraldehyde and incubated for 10 min at 50 °C. Loading buffer [0.5 M Tris/HCl, pH 8.5, 2% (w/v) SDS, 0.04% (w/v) Bromophenol Blue, 30% (v/v) glycerol and 100 mM ethanolamine] was added to block the cross-linking reaction, and assay mixtures were heated to 100 °C. A 10 μl sample of the solution was loaded on to Tris/acetate, pH 8.1, 3–8% (w/v) polyacrylamide gels (Invitrogen) and was electrophoresed for 75 min at 150 V at room temperature in 50 mM Tris, 50 mM Tricine, pH 8.2, and 0.1% (w/v) SDS, before being transferred on to nitrocellulose membranes for 1 h at 30 V in 25 mM Tris, 192 mM glycine, pH 9.3, and 20% (v/v) methanol. Leucotoxin complexes were characterized by immunoblotting

using affinity-purified anti-rabbit polyclonal antibodies and a horseradish-peroxidase-labelled goat anti-rabbit antibody using ECL<sup>®</sup> (enhanced chemiluminescence) detection (Amersham Biosciences). Apparent molecular masses of proteins were estimated according to Precision Plus<sup>®</sup> protein standards (Bio-Rad).

## RESULTS

### Choice of mutations

Biologically active cross-combinations of leucotoxins and recent advances have demonstrated the alternating locations of class S and class F components within the pore for the structurally related leucotoxin component sequences (Figure 1A) [23,33–35]. Examination of the crystal structures of HlgB and LukS-PV [34,35] revealed that residues Tyr-99, Asn-103, Gln-104, Arg-150, Thr-152, Ser-154, Arg-155, Asn-156, Thr-157 and Asn-158 are exposed to solvent and may be involved in protein–protein interactions within the functional pore (Figure 1A). All of these residues, as well as the solvent-exposed HlgA Thr-21 and Thr-28, were cysteine-substituted. Residues HlgB Tyr-99 and Gln-104 are located on a loop connecting strands 6 and 7, and residues HlgB Arg-150 and Asn-158 are located on a loop connecting strands 9 and 10 [34]. HlgA Thr-28, located on β-strand 3, was shown to play a key role in monomer oligomerization [18]. This residue of leucotoxin class S components aligns with His-35 of a given α-toxin monomer A (Figure 1B), which interacts with Tyr-101, Thr-161 and Asp-162 of monomer G. HlgB Tyr-99 aligns perfectly with Tyr-101 of α-haemolysin and was shown to be involved in contacts between monomers [36–38]. In parallel, HlgA Thr-21 (β-strand 1) might be close to HlgB Thr-157 and HlgB Asn-158 respectively [34,35].

### Heterodimer construction and purification

Figure 2 illustrates the purification steps of the covalent heterodimer HlgA T28C–HlgB N156C, which is representative of the highly purified dimers that were investigated in the present study. Lanes 2 and 6 of Figure 2 show HlgA T28C and HlgB N156C having similar apparent molecular masses as those of recombinant HlgA and HlgB (Figure 2, lane 7). These mutants may also have a tendency to form homodimers (64 or 74 kDa) in oxidizing conditions (Figure 2, lanes 3 and 5 respectively). Blocking the cysteine of one mutated component by DTDP favoured the thiol-exchange reaction of the labelled protein with the partner component, giving rise to a heterodimer with an apparent molecular mass of 68 kDa (Figure 2, lane 4). In contrast, when WT HlgA and HlgB were mixed together for 90 min at 23 °C, no dimerization appeared (Figure 2, lane 7). The heterodimer was detected by immunoblotting with both anti-HlgA and anti-HlgB antibodies (results not shown). Thiol-titrations with DTNB on to SDS-denatured proteins always gave significant yields (25–65%) of dimers including heterodimers useful for their purification, except for HlgB Y99C, HlgB R150C and HlgB N152C mutants challenged with either HlgA T21C or HlgA T28C, where one accessible cysteine was determined per protein (Lowry titration). Thus only some, but not all, of the cysteine residues remained accessible for disulphide bridge formation and failed to promote heterodimers. Purification of most heterodimers led to >99% pure complexes (Figure 2, lane 8).

### Cell-biological activities of heterodimers

The presence of cysteine mutations was first checked to be not deleterious for both haemolytic activities (HRBCs and RRBCs) compared with WT HlgA and HlgB (results not shown). In fact, HlgA T28C combined with HlgB was slightly less active than

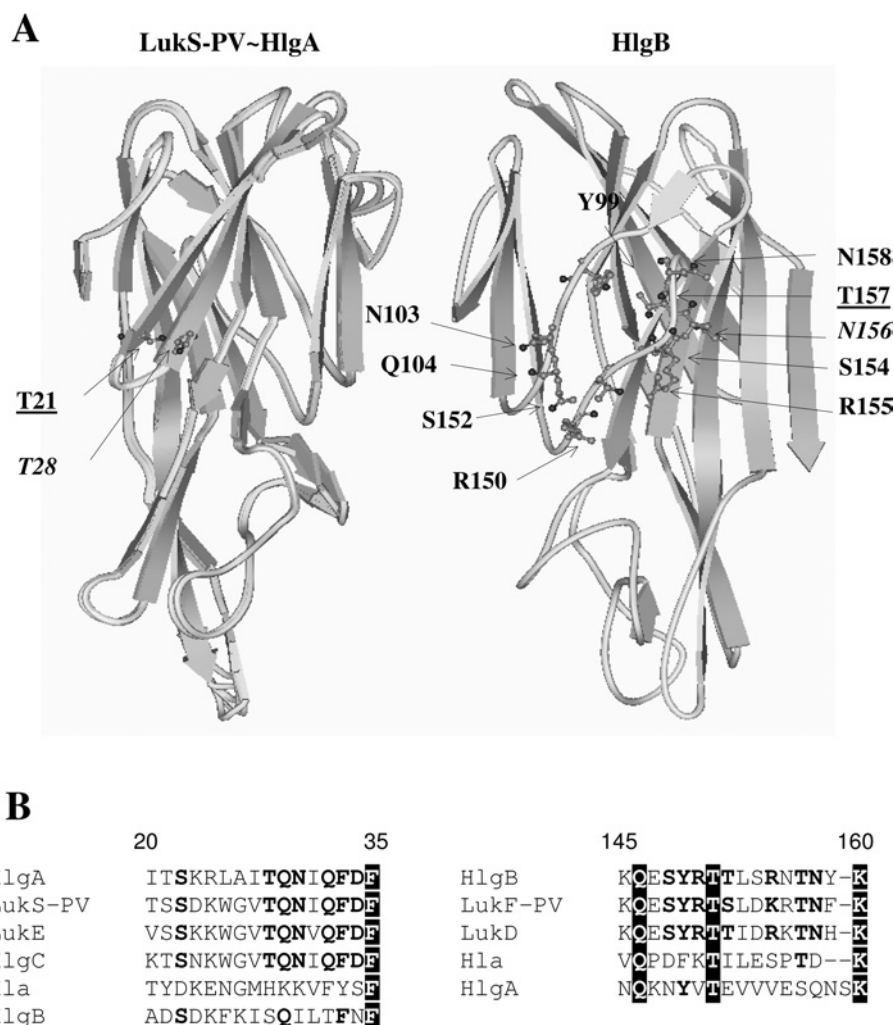


**Figure 1 Basic three-dimensional structures and sequence alignment of leucotoxins**

(A) Three-dimensional structures of LukS-PV (PDB code 1T5R; right-rear view) that might be comparable with that of HlgA and HlgB (PDB code 1LKF; left-rear view) and the location of the cysteine-substituted amino acids. Amino acids thought to interact each other are underlined and in italics respectively. (B) Sequence alignment of the *S. aureus* Hlg (GenBank<sup>®</sup> accession number X81586), PVL (GenBank<sup>®</sup> accession number X72700), LukE and LukD (GenBank<sup>®</sup> accession number Y13225) and  $\alpha$ -toxin (Hla, GenBank<sup>®</sup> accession number M90536). Conserved residues are shown in white on a black background, while common residues to bipartite leucotoxins are shown in bold; numbering of the amino acids is given on the basis of HlgA and HlgB respectively.

WT, and HlgB N103C combined with HlgA was approx. 10-fold less active on HRBC.

The lytic activities of heterodimers (20 nM) on to HRBCs, RRBCs and human PMNs are detailed in Table 1, and Figures 3 and 4. Pore-formation and ethidium bromide entry promoted into PMNs by heterodimers show that these cells are globally more sensitive than HRBCs. Dimer HlgA T21C–B N103C displays no lytic activity upon any cells tested. HlgA T21C–HlgB Q104C, HlgA T21C–HlgB R155C and HlgA T21C–HlgB N156C displayed decreased activities, judged to be approx. 20-fold greater than that of WT (see values in Table 1 for 1 nM WT) on HRBCs, RRBCs and human PMNs (Table 1, and Figures 3A and 4A). More curiously, HlgA T21C–HlgB S154C also had intermediate haemolytic activities (Table 1 and Figure 3A), but its leucocytolytic activity was comparable with that of the WT on PMNs (Figure 4A), indicating that behaviour against each cell was not uniform. Similarly, whereas HlgA T21C–HlgB N158C needs 18 min to lyse half of the HRBCs, its activity on RRBCs and PMNs was closer to that of WT (Table 1, and Figures 3A and 4A). HlgA

T21C–HlgB T157C and HlgA T21C–HlgB N158C seemed fully efficient against all of these PMNs.

Again, HlgA T28C–HlgB N103C had no lytic activity on cells and HlgA T28C–HlgB Q104C, HlgA T28C–HlgB S154C heterodimers harboured weak potentials to disrupt membranes of HRBCs, RRBCs and human PMNs, with both longer lag times and time courses to reach 100% lytic activity (Table 1, and Figures 3B and 4B). HlgA T28C–HlgB R155C and HlgA T28C–HlgB T157C were haemolytic, but they take more than 60 min to start haemolysis on HRBCs or RRBCs (Figure 3B and Table 1). The half-haemolysis time of HlgA T28C–HlgB N158C was 20 min, whereas HlgA T28C–HlgB N156C and HlgA T28C–HlgB N158C showed activity on HRBCs closer to that of the control, but with a 4 min lag time. On human PMNs, HlgA T28C–HlgB R155C generated pores as rapidly as the WT, while HlgA T28C–HlgB N158C revealed a decreased activity (Figure 4B). Only HlgA T28C–HlgB N156C and HlgA T28C–HlgB T157C had pore-forming activities between those of the WT and those of HlgA T28C combined with HlgB.

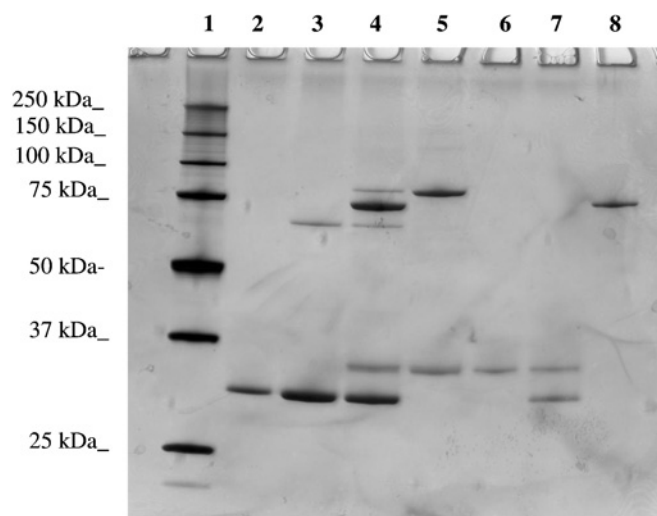


**Figure 2** Engineering and purification of the Hlg covalent heterodimer HlgA T28C-HlgB N156C

SDS/10–15% PAGE and silver staining. Lane 1, molecular ladder; lanes 2 and 6, HlgA T28C (0.3  $\mu$ g) and HlgB N156C (0.5  $\mu$ g) respectively, under reducing conditions; lanes 3 and 5, HlgA T28C (1  $\mu$ g) and HlgB N156C (0.8  $\mu$ g) respectively under oxidizing conditions; lane 4, HlgA T28C-HlgB N156C (1  $\mu$ g of the coupling reaction); lane 7, mixture of recombinant WT HlgA (0.2  $\mu$ g) and WT HlgB (0.15  $\mu$ g); lane 8, FPLC-purified HlgA T28C-HlgB N156C. Molecular-mass sizes are given in kDa.

**Table 1** Cytotoxic activities of Hlg covalent heterodimers

Results ( $t_{50}$ ) for HRBCs and RRBCs are times to reach half-haemolysis using 20 nM toxin; those for PMNs are times to reach 50% activity using 20 nM toxin. nd, not determined; na, not active.

Toxin	$t_{50}$ (min)		
	HRBCs	RRBCs	PMNs
WT	2.5	2.9/4.3	14.6
WT (1 nM)	24.3	nd	27.1
HlgA T21C-HlgB N103C	na	na	na
HlgA T21C-HlgB Q104C	9.8	9.4	20.0
HlgA T21C-HlgB S154C	10.8	7.9	16.3
HlgA T21C-HlgB R155C	> 60	23.0	22.7
HlgA T21C-HlgB N156C	> 60	13.7	20.0
HlgA T21C-HlgB T157C	8.8	3.1	14.6
HlgA T21C-HlgB N158C	18.0	4.9	17.3
HlgA T21C-HlgB N103C	na	na	na
HlgA T21C-HlgB Q104C	> 60	na	na
HlgA T21C-HlgB S154C	> 60	na	32.1
HlgA T21C-HlgB R155C	> 60	12.5	17.5
HlgA T21C-HlgB N156C	6.8	3.6	13.8
HlgA T21C-HlgB T157C	> 60	44.4	15.0
HlgA T21C-HlgB N158C	23.0	3.6	20.5

Comparable results were obtained for the calcium influx promoted by these toxins and heterodimers, which is known to occur before pore function [26,35]. HlgA T21C mutants may be inactive or partially active, but calcium channel opening induced by dimers HlgA T21C-HlgB T157C and HlgA T21C-HlgB N158C was comparable with that of WT Hlg (Figure 5). Calcium influx induced by HlgA T28C-HlgB N103C and HlgA T28C-HlgB Q104C were null or weak (Figure 5). HlgA T28C-HlgB S154C induced an intermediate activity, and the other heterodimers appeared closer to control (Figure 5B), which is likely to be because of the higher sensitivity of the Fluo-3 probe compared with ethidium bromide fluorescence. In fact, heterodimers engaging

positions far from Hlg N156C became less biologically active (Figures 3–5 and Table 1).

### Characteristics of ion channels formed by the heterodimers

All of the heterodimers able to permeabilize RBCs and LUVs (Tables 1 and 2) also opened similar ion conductive pores (Figure 6) as HlgA-HlgB does in planar lipid bilayers [22,26,39].

Heterodimers display similar electrophysiological pore properties, i.e. channel conductance and current voltage characteristics ( $I-V$ ) (Figure 6 and Table 2), which are very close to those of WT. In 100 mM KCl, pH 7.0, at +40 mV applied voltage, all of the pores normally stay open for most of the time (Figure 6), as do those formed by HlgA-HlgB [39] and  $\alpha$ -toxin [40]. Under such conditions, all of the dimers have similar mean conductance, ranging from 118 to 162 pS, similar to that of the WT, i.e. 128 pS (Figure 6 and Table 2). Some of them show a different propensity to open pores, as evidenced by the different rate of channel insertion, e.g. HlgA T28C-HlgB T157C was even more active. Furthermore, HlgA T21C-HlgB S154C shows a clear increase in current noise, possibly due to an increase in instability of the  $\beta$ -barrel [41], which may be due to a longer distance of interaction between key residues [24]. The  $I-V$  curve of the WT is markedly asymmetrical, i.e. there is a larger current flow at negative voltages [39]. An estimate of the extent of this non-linearity is given by the ratio  $I^-/I^+$  measured at 120 mV (Table 2). This ratio is identical for the Hlg and the heterodimers, indicating a similar charge distribution along the lumen of the channel. All of the toxins tested are slightly cation-selective as is the WT [23]. The cation/anion permeability ratio was determined as in Comai et al. [39] with a 20 mM *cis*-200 mM *trans* KCl gradient into 10 mM Hepes and 0.1 mM EDTA, pH 7.0. Thereafter, the concentration of the *trans* chamber was increased stepwise up to 200 mM KCl and the permeability values  $P^+/P^-$  were given by the ratio of cation and anion potential mobilities respectively. Under these conditions, WT Hlg had a cationic selectivity with a  $P^+/P^-$  of 1.4. The most active heterodimers tested, HlgA T21C-HlgB N156C and HlgA T28C-HlgB T157C were similar to WT or HlgA T28C-HlgB T157C pointed at 1.5, or HlgA T28C-HlgB N156C to 1.6. However, the pores formed by HlgA T28C-HlgB N158C and HlgA T21C-HlgB N158C harboured a higher cationic selectivity of 2.0 and 2.1 respectively.

### Oligomer analysis

To screen the amount and stoichiometry of oligomers formed by heterodimers and inserted into cell membranes, these oligomers were recovered from membranes and stabilized by a chemical cross-linking to escape their degradation when released from membranes. As shown in Figure 7 (lane 3), 4 ng of purified HlgA and HlgB at nanomolar concentrations which were mixed together and incubated for 10 min with 0.3 mM glutaraldehyde produced concatemers of the two proteins where at least dodecamers could be distinguished on SDS/3–8% (w/v) PAGE. The use of 3 mM glutaraldehyde in such assays alters the signal by producing aggregates (Figure 7, lane 4). No material cross-reacting with antibodies were detected from lysed PMNs (Figure 7, lane 1). HlgA and HlgB in solution produce low amounts of homodimers, but those produced are stable to either SDS treatment (lane 2) or application to PMNs and retrieval after saponin treatment (lane 5) and boiling. Boiling is also necessary when oligomers contained in PMNs lysates are treated with 3 mM glutaraldehyde. Absence of boiling actually reveals a bulky signal of probable non-denatured oligomers (octamers?) (Figure 7, lane 6). In fact, even if a Schiff reaction may also be promoted by glutaraldehyde, cross-linking

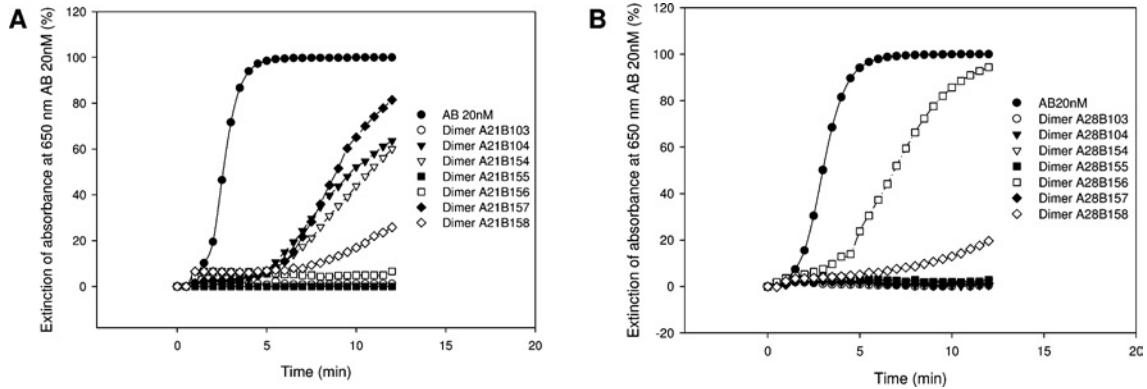


**Figure 3** HlgA–HlgB heterodimers induce variable haemolytic activities in HRBCs compared with the WT toxin

HRBCs were incubated in the presence of 20 nM heterodimers obtained by combining HlgA T21C (A) or HlgA T28C (B). The haemolytic activity was monitored by following the decrease in absorbance at 650 nm. Kinetics were then normalized as a function of the 100% of haemolysis obtained for the control, as described in the Materials and methods section. Dimers are abbreviated to A (HlgA) or B (HlgB) and the positions of residues that were mutated to cysteine.

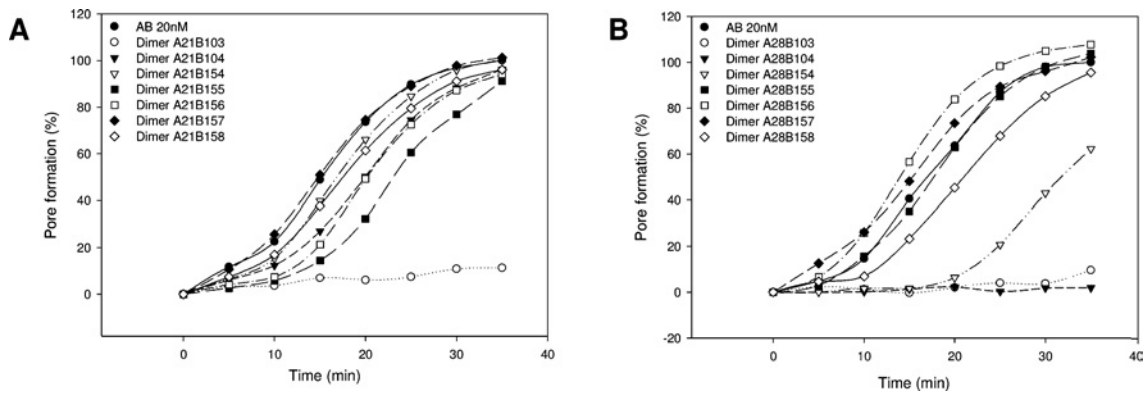


**Figure 4** Pore-forming activity and ethidium bromide entry into human PMNs are induced by the HlgA–HlgB heterodimers

Human PMNs were incubated in the presence of 20 nM heterodimers obtained by combining HlgA T21C (A) or HlgA T28C (B), and formation of pores was followed by the entry of ethidium bromide and its combination with nucleic acids, as described in the Materials and methods section. The WT HlgA–HlgB leucotoxin, applied at 20 nM, was used as a control. Dimers are abbreviated to A (HlgA) or B (HlgB) and the positions of residues that were mutated to cysteine.

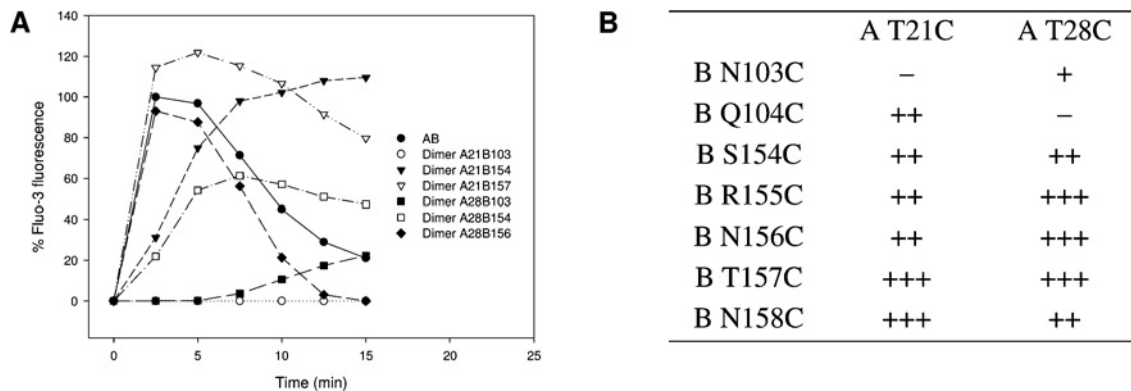


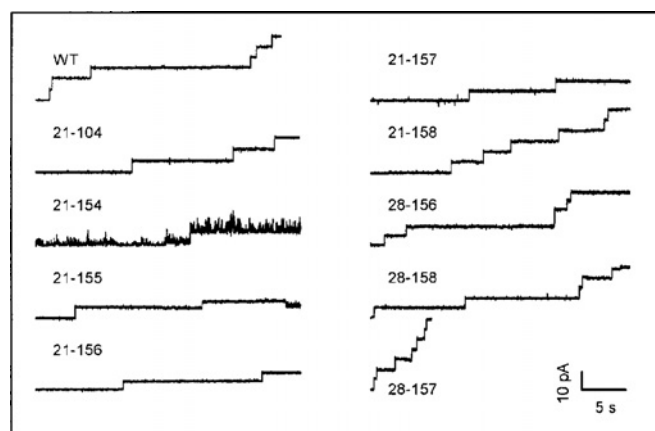
**Figure 5** HlgA–HlgB heterodimers are responsible for different  $\text{Ca}^{2+}$  influxes into human PMNs as evaluated by flow cytometry

(A) Each heterodimer and the control (HlgA plus HlgB) were used at 20 nM. Dimers HlgA T21C–HlgB N158C and HlgA T28C–HlgB R155C activities were similar to those of HlgA T21C–HlgB T157C and HlgA T28C–HlgB N156C. Dimers HlgA T21C–HlgB Q104C, HlgA T21C–HlgB R155C and HlgA T21C–HlgB N156C activities were intermediate, similar to those of HlgA T21C–HlgB S154C and HlgA T28C–HlgB S154C. Dimer HlgA T28C–HlgB Q104C activity was null like that of HlgA T21C–HlgB N103C. Dimers are abbreviated to A (HlgA) or B (HlgB) and the positions of residues that were mutated to cysteine. (B) Compared calcium entries induced by all purified heterodimers, from serial data as in (A). +++, similarly as active as the control (fluorescence greater than 70% of the control at 5 min incubation); ++, intermediate activity (fluorescence between 20 and 70% of the control at 5 min incubation); +, weak activity (fluorescence less than 20% of the control at 5 min incubation and greater than 10% at 15 min of incubation); –, no calcium entry.

**Table 2** Characterization of the permeabilization activity on model membranes

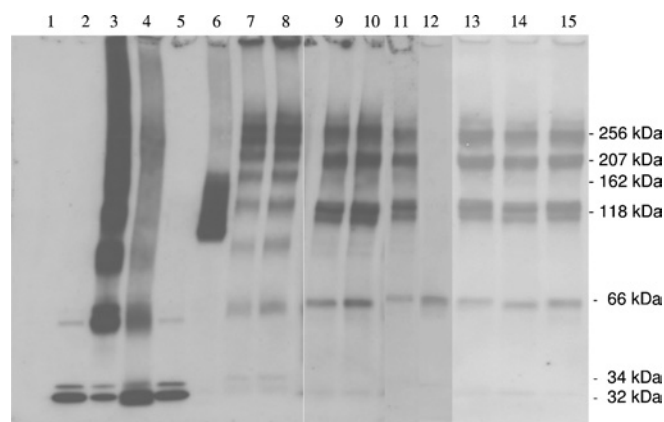
Permeabilization activity on LUVs and ion transport properties of the channels formed by Hlg and their stabilized heterodimers in planar lipid bilayers were determined. Values of the aqueous pore radii were deduced from the inflexion point of the curves given by FCS variations for PMNs treated with PEG molecules and the different heterodimers [27]. Permeabilizing activity of the heterodimers on LUVs comprising phosphatidylcholine/choline (1:1 molar ratio) are reported as the time(s) necessary to cause 40% calcein release ( $t_{40}$ ) at 50 nM toxin. Results are means for at least three different experiments. The final concentration of lipids was 5  $\mu$ M. Single-channel conductance was obtained at +40 mV. Values are means  $\pm$  S.D. obtained from traces such as those in Figure 6. The number of events used, taken from three to eight different experiments, ranged from 32 to 608. The ratio between the ion current flowing through a single channel at negative ( $I^-$ ) and positive ( $I^+$ ) voltages was measured at 120 mV and 100 mM KCl. Values are means  $\pm$  S.E.M. for three to eight different experiments. Activity on planar lipid bilayers is expressed as the number of pores obtained after 3 min of toxin addition. Toxin concentration in nM is given in parentheses. nd, not determined; na, not active.

Toxin	Aqueous pore radius of PMNs (nm)	Calcein release (s)	Conductance (pS)	$I^-/I^+$	Planar lipid bilayer activity
WT	1.12	57	128 $\pm$ 13	2.7	18 (2)
HlgA T21C–HlgB N103C	nd	na	–	–	0 (303)
HlgA T21C–HlgB Q104C	nd	na	162 $\pm$ 7	2.4	1 (60)
HlgA T21C–HlgB S154C	nd	na	120	–	0 (71)
HlgA T21C–HlgB R155C	nd	na	162	–	0 (250)
HlgA T21C–HlgB N156C	1.12	na	126 $\pm$ 17	3.2	3 (150)
HlgA T21C–HlgB T157C	1.12	579	133 $\pm$ 13	2.9	120 (3)
HlgA T21C–HlgB N158C	1.12	879	144 $\pm$ 14	2.6	31 (2)
HlgA T21C–HlgB N103C	nd	na	–	–	0 (400)
HlgA T21C–HlgB Q104C	nd	na	–	–	0 (280)
HlgA T21C–HlgB S154C	nd	na	–	–	0 (84)
HlgA T21C–HlgB R155C	1.12	na	–	–	0 (248)
HlgA T21C–HlgB N156C	1.12	182	118 $\pm$ 12	3.3	32 (9)
HlgA T21C–HlgB T157C	1.12	211	137 $\pm$ 19	3	21 (2)
HlgA T21C–HlgB N158C	1.12	20	130 $\pm$ 15	2.6	25 (3)

**Figure 6** Formation of ion channels in planar lipid bilayers by Hlg and dimers

Representative stepwise current increases corresponding to the opening of single ion channels of Hlg WT and all of the active heterodimers as indicated on the left of each trace. Each protein was added to the *cis* side at the concentrations reported in brackets of Table 2. The applied voltage was +40 mV in all cases. The height of each step was used to calculate the conductance of that pore as reported in Table 2.

probably occurs in our assays through the additional reaction of basic residues (R-NH<sub>2</sub>) on to hydrazide groups. Because of a 100-fold excess of cell proteins in lysates, the observed oligomers are assumed to be preformed oligomers, because, if spontaneously generated in solution, they would be dispersed by cross-linking with other cell proteins. Figure 7, lane 3 represents 4 ng of the previously applied HlgA and HlgB in solution, whereas lane 7 represents 15 ng of each of the previously applied HlgA and HlgB issued from membrane-inserted oligomers. Thus a significant yield of recovery for oligomers can be assumed, since non-bound proteins were lost in the recovery of oligomers and intermediates (Figure 7, lanes 7–11). Besides a minimal duration of 10 min for the saponin treatment, temperature does not much influence cholesterol extraction (Figure 7, lanes 7 and 8). Under these condi-

**Figure 7** HlgA and HlgB and heterodimer oligomers formed in solution or after their insertion into human PMN membranes

Oligomers were analysed by SDS/3–8% (w/v) PAGE and were revealed by immunoblotting with anti-LukS-PV and anti-LukF-PV affinity-purified rabbit antibodies with WT. Lane 1, PMNs only; lane 2, HlgA and HlgB (0.2 ng each) were mixed for 1 h at room temperature and analysed; lane 3, 4 ng of each HlgA and HlgB was concatenated in solution with 0.3 mM glutaraldehyde; lane 4, same experiment as in lane 3, but with 3 mM glutaraldehyde; lane 5, HlgA and HlgB were applied to human PMNs and retrieved after saponin treatment, but without glutaraldehyde; lane 6, HlgA (15 ng) and HlgB (15 ng) oligomers were applied to human PMNs and retrieved after saponin and glutaraldehyde treatments, before being electrophoresed without boiling; lanes 7 and 8, temperature, 0 °C or 23 °C respectively, of the saponin treatment did not affect the retrieving of oligomers that were boiled after the glutaraldehyde treatment; lanes 9–11, 30 ng of heterodimers HlgA T28C–HlgB N156C, HlgA T28C–HlgB T157C and HlgA T21C–HlgB R155C respectively were applied to human PMNs, and oligomers were prepared as in lane 8 and show octamers, hexamers, tetramers and dimers as well as monomers in minor quantities. Any heterodimers with full or medium activities produced similar oligomers (not shown); lane 12, HlgA T28C–N103C (or HlgA T28C–Q104C, not shown) failed to promote oligomers under the same conditions as in lanes 7 to 11; lanes 13, 14 and 15, oligomers obtained from other active heterodimers: HlgA T21C–HlgB N156C, HlgA T21C–HlgB T157C and HlgA T21C–HlgB N158C. Molecular-mass sizes are given in kDa.

tions comprising glutaraldehyde cross-linking, octamers and intermediates with decreasing intensities can be seen for WT toxin or active heterodimers (Figure 7, lanes 7–11 and 13–15). Finally,

the inactive heterodimer HlgA T28C–HlgB N103C shows only a low dimer band, probably because of oligomerization properties (Figure 7, lane 12).

## DISCUSSION

We developed a new strategy based on thiol-protection/activation to obtain stabilized heterodimers of *S. aureus* leucotoxins and to learn more about monomer–monomer interactions of leucotoxins that are associated with pathologies such as furuncles, pneumonia, antibiotic-associated diarrhoea and impetigo [1]. Native leucotoxins are devoid of cysteine residues, hence mutations took into account the predicted accessibility of residues [34,35,37]. DTDP was a useful protective group for a given cysteine mutant to favour the thiol-exchange reaction and heterodimerization when bringing the second protein with another thiol group. Dependent on combinations, yields up to 65% were obtained. However, dimers do not form at any combination of mutants, and in the case of mutations at positions 99, 150, 152 of HlgB and combined with both HlgA T21C and T28C, no significant amount of dimers was obtained. In fact, HlgB Tyr-99 aligns with Tyr-101 of  $\alpha$ -toxin, and, with respect to a strictly similar model, we would expect activity with a dimer based on HlgA T28C that aligns with His-35 of  $\alpha$ -toxin [18,37], since both His-35 and Thr-28 of leucotoxin class S proteins are very important for oligomerization of these toxins [18,35,36,38]. These observations suggest that monomer–monomer interactions between  $\alpha$ -toxin and leucotoxin monomers might be different. Residue location was probably too low in the HlgB structure when challenging heterodimers with HlgB Arg-150 and Thr-152 (Figure 1), underlining limits in the flexibility of the HlgB loop supporting these residues.

In fact, heterodimers harboured ionic properties as HlgA, but hydrophobic properties were close to HlgB. These aspects made profit in order to obtain highly purified dimers. Among the 14 covalent heterodimers of HlgA and HlgB, those including HlgB N103C are inactive in the different assays though these heterodimers develop haemolysis within 24 h at concentrations that allow straight haemolysis in the case of active heterodimers. The oligomerization property of these dimers was dramatically affected (Figure 7). It is noteworthy that residue 103 of HlgB is located in the triangle region that may play a key role in the unfolding of the stem during pore formation [34,37].

Because of the non-specific binding of HlgA on to target cells [18], the binding properties of heterodimers are difficult to appreciate and are probably complex with interactions with a membrane-specific ligand, with phospholipids and with an adjacent monomer. The haemolytic potential of other heterodimers remained more or less efficient, despite that the onset was longer than for the WT toxin (Figure 3 and Table 1). Whereas  $\text{Ca}^{2+}$  induction always took place very rapidly into PMNs, we noticed that to reach the maxima of haemolysis, a longer time was needed for heterodimers to reach maximal ethidium bromide influx into PMNs, compared with the WT toxin (Figures 4 and 5). Since prepore formation is required for  $\text{Ca}^{2+}$  induction into PMNs [42], the difference in delays for haemolysis can only be explained by a longer time to reach functional pore formation for heterodimers into red blood cells. HlgA T21C–HlgB Q104C is more active on all membranes than HlgA T28C–HlgB Q104C, probably indicating a better configuration of the disulphide bridge (Figures 3–5). Such a difference concerning residues located on neighbour  $\beta$ -strands may reflect the necessary good positioning of this loop to allow the stem to be functional. Some flexibility in the final structural accommodation of the HlgB loop when the stem domain refolds into a  $\beta$ -hairpin on to human PMNs at least may

be indicated by heterodimers that harbour intermediate biological activities (Figure 4). Pores formed by these dimers have aqueous pore radii, conductance and ionic selectivity similar to those of the WT toxin (Table 2), but concentrations needed to obtain such pores were often higher than for WT, suggesting that the dynamics of pore formation are affected.

The most active heterodimers are HlgA T28C–HlgB N156C and HlgA T21C–HlgB T157C or –HlgB N158C (Figures 3–7) with pore characteristics similar to that of WT toxin. Only one heterodimer, HlgA T21C–HlgB N158C harbours a higher cationic selectivity, a high conductance at 144 pS and a high activity on planar lipid bilayers (Table 2). This may indicate that the loop of HlgB, supporting residues 150–160, is now in a different orientation, which modifies locations of charges inside the lumen of the pore thus inducing a positive influence on the selectivity. This strongly suggests that these dimers finally preserve correct monomer–monomer interaction, strand refolding kinetics of the stem, positioning of the  $\beta$ -hairpin to form the pore and finally ionic selectivity and diameter of the pore (Table 2). Moreover, any of the active heterodimers form octamers and may be other lower oligomers within the membrane of target cells (Figure 7, lanes 9–11). Therefore these covalently rigidified but active heterodimers probably mimic one (i.e. S–F) of the two interprotomer interfaces that probably occurs in the WT leucotoxin, and conserve potential to promote pore assembly by dimer–dimer interactions through the formation of the second (F–S) interface.

As class S components of leucotoxins bind first to a yet non-defined membrane ligand, and then allow the secondary binding of the F component, the synthesis of S–F heterodimers certainly modify some constants. The resulting kinetics of the induced  $\text{Ca}^{2+}$  influx and pore formation of active dimers remained, however, similar to those of the WT toxin. However, in the case of a membrane ligand, one can assert that the structural conformation of HlgA and HlgB monomers within the bound heterodimer efficiently provides an efficient accommodation compatible for binding and to achieve the prepore as for cholesterol-dependent cytolysins [43].

In conclusion, the challenge of leucotoxin heterodimers found that (i) protein–protein interfaces found within leucotoxins may not be strictly identical with those found in the related  $\alpha$ -toxin, (ii) red blood cell membranes are not strictly equivalent to PMN membranes when considering heterodimers and may influence the kinetic of stem insertion and function, (iii) the loop corresponding to residues 150–158 of HlgB is involved in interactions with residues located on  $\beta$ -strand 2 of HlgA, (iv) the plasticity of this loop is such that it might tolerate sequence microheterogeneities and this may account for the different possible combinations observed for the assembly of the bipartite leucotoxins [33], (v) the biologically active heterodimers can be considered to be functional units of leucotoxin pores and their structures can accommodate further oligomerization and functional pores as for the WT toxin, and (vi) these heterodimers might constitute a valuable approach for unravelling the structure of assembled leucotoxins while they look more unstable as pores outside membranes than  $\alpha$ -toxin [21]. Accordingly, and together with other studies, the three-dimensional structure of one of these active heterodimers should help to reconstitute the S–F interface.

This work was supported by a grant from the Direction de la Recherche et des Etudes Doctorales (UPRES EA-3432) and partially supported by Fondazione Cariverona (Bando 2004, Integrazione tra Tecnologia e Sviluppo di Settore). We thank A. Gropuzzo, R. Girardot and M. Couturier for technical support. O.J. was supported by grant from a research convention (project StaWars) between Provincia Autonoma di Trento (Italy) and Université Louis Pasteur, and the Conseil Régional d'Alsace. G.V. was supported by a Ph.D. grant from the University of Verona (Italy).

## REFERENCES

- Prévost, G., Mourey, L., Colin, D. A., Monteil, H., Dalla Serra, M. and Menestrina, G. (2005)  $\alpha$ -Toxin and  $\beta$ -barrel pore-forming toxins (leucocidins,  $\alpha$ -,  $\gamma$ -, and  $\delta$ -cytolysins) of *Staphylococcus aureus*. In *The Comprehensive Sourcebook of Bacterial Protein Toxins* (Alouf, J. E. and Popoff, M. R., eds.), pp. 588–605, Academic Press, London
- Rosjohn, J., Feil, S. C., McKinstry, W. J., Tweten, R. K. and Parker, M. W. (1997) Structure of a cholesterol-binding, thiol-activated cytolysin and a model of its membrane form. *Cell* **89**, 685–692
- Moayeri, M. and Leppla, S. H. (2004) The roles of anthrax toxin in pathogenesis. *Curr. Opin. Microbiol.* **7**, 19–24
- Aktorjes, K. (1994) Clostridial ADP-ribosylating toxins: effects on ATP and GTP-binding proteins. *Mol. Cell. Biochem.* **138**, 167–176
- Thelestam, M., Olofsson, A., Blomqvist, L. and Hebert, H. (1991) Oligomerization of cell-bound staphylococcal  $\alpha$ -toxin in relation to membrane permeabilisation. *Biochim. Biophys. Acta* **1062**, 245–254
- Walker, B., Krishnaswamy, M., Zorn, L. and Bayley, H. (1992) Assembly of the oligomeric membrane pore formed by Staphylococcal  $\alpha$ -hemolysin examined by truncation mutagenesis. *J. Biol. Chem.* **267**, 21782–21786
- Vécsey-Sémjen, B., Lesieur, C., Mollby, R. and van der Goot, F. G. (1997) Conformational changes due to membrane binding and channel formation by staphylococcal  $\alpha$ -toxin. *J. Biol. Chem.* **272**, 5709–5717
- Vécsey-Sémjen, B., Möllby, R. and van der Goot, F. G. (1996) Partial C-terminal unfolding is required for channel formation by staphylococcal  $\alpha$ -toxin. *J. Biol. Chem.* **271**, 8655–8660
- Tilley, S. J., Orlova, E. V., Gilbert, R. J., Andrew, P. W. and Saibil, H. R. (2005) Structural basis of pore formation by the bacterial toxin pneumolysin. *Cell* **121**, 247–256
- Miller, C. J., Elliott, J. L. and Collier, R. J. (1999) Anthrax protective antigen: prepore-to-pore conversion. *Biochemistry* **38**, 10432–10441
- Sellman, B. R., Kagan, B. L. and Tweten, R. K. (1997) Generation of a membrane-bound, oligomerized pre-pore complex is necessary for pore formation by *Clostridium septicum*  $\alpha$  toxin. *Mol. Microbiol.* **23**, 551–558
- Hotze, E. M., Wilson-Kubalek, E. M., Rosjohn, J., Parker, M. W., Johnson, A. E. and Tweten, R. K. (2001) Arresting pore formation of a cholesterol-dependent cytolysin by disulfide trapping synchronizes the insertion of the transmembrane  $\beta$ -sheet from a prepore intermediate. *J. Biol. Chem.* **276**, 8261–8268
- Czajkowsky, D. M., Hotze, E. M., Shao, Z. and Tweten, R. K. (2004) Vertical collapse of a cytolysin prepore moves its transmembrane  $\beta$ -hairpins to the membrane. *EMBO J.* **23**, 3206–3215
- Ramachandran, R., Tweten, R. K. and Johnson, A. E. (2005) The domains of a cholesterol-dependent cytolysin undergo a major FRET-detected rearrangement during pore formation. *Proc. Natl. Acad. Sci. U.S.A.* **102**, 7139–7144
- Parker, M. W. and Feil, S. C. (2005) Pore-forming protein toxins: from structure to function. *Prog. Biophys. Mol. Biol.* **88**, 91–142
- Ramachandran, R., Tweten, R. K. and Johnson, A. E. (2004) Membrane-dependent conformational changes initiate cholesterol-dependent cytolysin oligomerization and intersubunit  $\beta$ -strand alignment. *Nat. Struct. Mol. Biol.* **11**, 697–705
- Hotze, E. M., Heuck, A. P., Czajkowsky, D. M., Shao, Z., Johnson, A. E. and Tweten, R. K. (2002) Monomer–monomer interactions drive the prepore to pore conversion of a  $\beta$ -barrel-forming cholesterol-dependent cytolysin. *J. Biol. Chem.* **277**, 11597–11605
- Meunier, O., Ferreras, M., Supersac, G., Hoepfer, F., Baba-Moussa, L., Monteil, H., Colin, D. A., Menestrina, G. and Prévost, G. (1997) A predicted  $\beta$ -sheet from class S components of staphylococcal  $\gamma$ -hemolysin is essential for the secondary interaction of the class F component. *Biochim. Biophys. Acta* **1326**, 275–286
- Sugawara-Tomita, N., Tomita, T. and Kamio, Y. (2002) Stochastic assembly of two-component staphylococcal  $\gamma$ -hemolysin into heteroheptameric transmembrane pores with alternate subunit arrangements in ratios of 3:4 and 4:3. *J. Bacteriol.* **184**, 4747–4756
- Miles, G., Movileanu, L. and Bayley, H. (2002) Subunit composition of a bicomponent toxin: staphylococcal leukocidin forms an octameric transmembrane pore. *Protein Sci.* **11**, 894–902
- Jayasinghe, L. and Bayley, H. (2005) The leukocidin pore: evidence for an octamer with four LukF subunits and four LukS subunits alternating around a central axis. *Protein Sci.* **14**, 2550–2561
- Ferreras, M., Hoper, F., Dalla Serra, M., Colin, D. A., Prévost, G. and Menestrina, G. (1998) The interaction of *Staphylococcus aureus* bi-component  $\gamma$ -hemolysins and leucocidins with cells and lipid membranes. *Biochim. Biophys. Acta* **1414**, 108–126
- Viero, G., Cunnaccia, R., Prévost, G., Werner, S., Monteil, H., Keller, D., Joubert, O., Menestrina, G. and Dalla Serra, M. (2006) Homologous versus heterologous interactions in the bicomponent staphylococcal  $\gamma$ -hemolysins pore. *Biochem. J.* **394**, 217–225
- Jayasinghe, L., Miles, G. and Bayley, H. (2006) Role of the amino latch of staphylococcal  $\alpha$ -hemolysin in pore formation: a co-operative interaction between the N terminus and position 217. *J. Biol. Chem.* **281**, 2195–2204
- Valeva, A., Palmer, M. and Bhakdi, S. (1997) Staphylococcal  $\alpha$ -toxin: formation of the heptameric pore is partially cooperative and proceeds through multiple intermediate stages. *Biochemistry* **36**, 13298–13304
- Werner, S., Colin, D. A., Coraiola, M., Menestrina, G., Monteil, H. and Prévost, G. (2002) Retrieving biological activity from LukF-PV mutants combined with different S components implies compatibility between the stem domains of these staphylococcal bicomponent leucotoxins. *Infect. Immun.* **70**, 1310–1318
- Baba-Moussa, L., Werner, S., Colin, D. A., Mourey, L., Pédelacq, J. D., Samama, J. P., Sanni, A., Monteil, H. and Prévost, G. (1999) Decoupling the  $\text{Ca}^{2+}$ -activation from the pore-forming function of the bi-component Pantón–Valentine leucocidin in human PMNs. *FEBS Lett.* **461**, 280–286
- Ellman, G. and Lysko, H. (1979) A precise method for the determination of whole blood and plasma sulfhydryl groups. *Anal. Biochem.* **93**, 98–102
- Malovrh, P., Viero, G., Dalla Serra, M., Podlesek, Z., Lakey, J. H., Macek, P., Menestrina, G. and Anderluh, G. (2003) A novel mechanism of pore formation: membrane penetration by the N-terminal amphipathic region of equinatoxin. *J. Biol. Chem.* **278**, 22678–22685
- Tejuca, M., Dalla Serra, M., Ferreras, M., Lanio, M. E. and Menestrina, G. (1996) Mechanism of membrane permeabilization by sticholysin I, a cytolysin isolated from the venom of the sea anemone *Stichodactyla helianthus*. *Biochemistry* **35**, 14947–14957
- Colin, D. A., Mazurier, I., Sire, S. and Finck-Barbançon, V. (1994) Interaction of the two components of leukocidin from *Staphylococcus aureus* with human polymorphonuclear leukocyte membranes: sequential binding and subsequent activation. *Infect. Immun.* **62**, 3184–3188
- Gauduchon, V., Werner, S., Prévost, G., Monteil, H. and Colin, D. A. (2001) Flow cytometric determination of Pantón–Valentine leucocidin S component binding. *Infect. Immun.* **69**, 2390–2395
- Dalla Serra, M., Coraiola, M., Viero, G., Comai, M., Potrich, C., Ferreras, M., Baba-Moussa, L., Colin, D. A., Menestrina, G., Bhakdi, S. and Prévost, G. (2005) *Staphylococcus aureus* bicomponent  $\gamma$ -hemolysins, HlgA, HlgB, and HlgC, can form mixed pores containing all components. *J. Chem. Inf. Model.* **45**, 1539–1545
- Olson, R., Nariya, H., Yokota, K., Kamio, Y. and Gouaux, E. (1999) Crystal structure of staphylococcal LukF delineates conformational changes accompanying formation of a transmembrane channel. *Nat. Struct. Biol.* **6**, 134–140
- Guillet, V., Roblin, P., Werner, S., Coraiola, M., Menestrina, G., Monteil, H., Prévost, G. and Mourey, L. (2004) Crystal structure of leukocidin S component: new insight into the Staphylococcal  $\beta$ -barrel pore-forming toxins. *J. Biol. Chem.* **279**, 41028–41037
- Jursch, R., Hildebrand, A., Hobom, G., Trantum-Jensen, J., Ward, R., Kehoe, M. and Bhakdi, S. (1994) Histidine residues near the N terminus of staphylococcal  $\alpha$ -toxin as reporters of regions that are critical for oligomerization and pore formation. *Infect. Immun.* **62**, 2249–2256
- Song, L., Hobaugh, M. R., Shustak, C., Cheley, S., Bayley, H. and Gouaux, J. E. (1996) Structure of staphylococcal  $\alpha$ -hemolysin, a heptameric transmembrane pore. *Science* **274**, 1859–1866
- Walker, B. and Bayley, H. (1995) Key residues for membrane binding, oligomerization, and pore forming activity of staphylococcal  $\alpha$ -hemolysin identified by cysteine scanning mutagenesis and targeted chemical modification. *J. Biol. Chem.* **270**, 23065–23071
- Comai, M., Dalla Serra, M., Coraiola, M., Werner, S., Colin, D. A., Monteil, H., Prévost, G. and Menestrina, G. (2002) Protein engineering modulates the transport properties and ion selectivity of the pores formed by staphylococcal  $\gamma$ -haemolysins in lipid membranes. *Mol. Microbiol.* **44**, 1251–1267
- Menestrina, G. (1986) Ionic channels formed by *Staphylococcus aureus*  $\alpha$ -toxin: voltage-dependent inhibition by divalent and trivalent cations. *J. Membr. Biol.* **90**, 177–190
- Cheley, S., Braha, O., Lu, X., Conlan, S. and Bayley, H. (1999) A functional protein pore with a “retro” transmembrane domain. *Protein Sci.* **8**, 1257–1267
- Nguyen, V. T., Higuchi, H. and Kamio, Y. (2002) Controlling pore assembly of staphylococcal  $\gamma$ -haemolysin by low temperature and by disulphide bond formation in double-cysteine LukF mutants. *Mol. Microbiol.* **45**, 1485–1498
- Gilbert, R. J. (2005) Inactivation and activity of cholesterol-dependent cytolysins: what structural studies tell us. *Structure* **13**, 1097–1106